Journal of Bioengineering and Biomedical Science

Kathoon Sanofer S et al., J Bioengineer & Biomedical Sci 2018, 8:3
DOI: 10.4172/2155-9538.1000254

Research Article Open Access

Lithium Zinc Chloride Nanoparticles by Simple Co-Precipitation Method

Kathoon Sanofer S[1], Madhumitha B[1], Ponsurya P[2], Abbas Shahul Hameed BH[3], Mikila Vaahini K[4], Sekar N[6], Nagarani N[5] and Ayeshamariam A[6*]

[1]*Department of Instrumentation Control, St. Joseph's College of Engineering, Chennai-119, India*

[2]*Department of Mechanical Engineering, Loyola ICAM College of Engineering and Technology, Nungambakkam, Chennai-34, India*

[3]*Department of Mechanical Engineering, SMR East Coast College of Engineering and Technology, Somanathapattinam, Thanjavur District, 614 612, India*

[4]*Department of Electrical and Electronics Engineering, St. Joseph's College of Engineering, Chennai-119, India*

[5]*Department of Physics, Sree Meenakshi Government Arts College for Women, Madurai, 625002, India*

[6]*Department of Physics, Khadir Mohideen College, Adirampattinam, 614701, India*

[*]**Corresponding author:** Ayeshamariam A, Department of Physics, Khadir Mohideen College, Adirampattinam, 614701, India, Tel: +91-9486738806; E-mail: aismma786@gmail.com

Received Date: August 17, 2018; **Accepted Date:** August 24, 2018; **Published Date:** August 31, 2018

Abstract

Lithium zinc chloride nanoparticles were prepared by simple co-precipitation method and characterized by using X-ray Diffractometer to find the crystal structure and its size. Morphological studies confirm the shape and agglomerations of individual nanoparticles. Optical photoluminescence studies gives its emission and excitation wavelengths. Further this particle will be used to prepare battery device of energy storing applications.

Keywords: $LiZnCl_4$; Co precipitation; XRD; Optical studies

Introduction

Nanoparticulate electrodes, such as Li_2ZnCl_4, have unique advantages over their microparticulate counterparts for the applications in Li-ion batteries because of the shortened diffusion path and access to nonequilibrium routes for fast Li incorporation, thus radically boosting power density of the electrodes [1-3]. Li intercalation occurs locally in a single nanoparticles of such materials remains unresolved because real-time observation at such a fine scale is still lacking which was well agreement with the JCPDS file number 86-1806. Many researchers reported visualization of local Li intercalation via solid-solution transformation in individual Li_2ZnCl_4 nanoparticles, enabled by probing sub-angstrom changes in the lattice spacing *in situ*. The real-time observation reveals inhomogeneous intercalation, accompanied with an unexpected reversal of Li concentration at the nanometer scale. The origin of the reversal phenomenon is elucidated through phase-field simulations, and it is attributed to the presence of structurally different regions that have distinct chemical potential functions. The findings from this study provide a simple perspective on the structural and morphological properties of synthesized Li_2ZnCl_4 nanoparticles by using sol-gel method [4-6].

Materials and Methods

For synthesis of nano composites using analytical grade I molar solution in 25 ml of Lithium chloride MW (42.394 gm/mol) (1.0599 gm) with 0.05 molar solution of Zinc chloride Molar mass (136.286 g/mol) (0.17 gm) and H_2O_2 liquid (10 vol%) was stirred with total volume of 25 ml deionised water without further purification. By using magnetic stirrer the above solution was stirred for one hr continuously. Milk white solution was placed on the hot plate and raise the temperature above 100°C until we get the fine powder. It is very simple co-precipitation method to prepare the particles. Then the prepared nano composites were oven dried at 60°C for 2 hours and finally annealed to the temperatures of 200°C for continuous 2 hours under static air atmosphere [7,8]. The as prepared and annealed nano composites were taken for further characterisation.

Characterization

The nanoparticles confirmation were carried out by powder X-ray diffraction (XRD) X-ray diffractometer (XRD) with monochromation CuKα target (1.5406A°) at a scan rate of 20/min. Scanning electron microscope (SEM) work on the calcined powders were performed under Scanning Electron Microscope Cambridge 53400N. The photoluminescence (PL) spectra were obtained from fluoro-spectrophotometer (Cary Eclipse) by using 280 nm line of Xe lamp as excitation source.

Results and Discussion

Structural studies (XRD)

The structure of the crystallites of the thin films developed is to be studied to assess whether the films could be used for the intended applications. The X-ray Diffraction (XRD) technique is a very powerful tool for the crystal structure determination. X-rays are a form of electromagnetic radiation, which can be diffracted by the atom bearing planes of a crystal. Using X-ray diffraction, information about the crystal structure can be obtained from the positions and intensities of the diffracted beams. Taking that the scattering centers (atoms) are located in a set of crystal planes whose directional properties are described by the Miller indices hkl, the distance between the planes (d_{hkl}) can be related to the scattering angle (θ_{hkl}) between the planes and the incoming beam, by the Bragg equation [9].

$2d_{hkl}\sin\theta_{hkl}=n\lambda$

Where λ is the wavelength of the X-rays and n is the order of diffraction. For diffraction it is also necessary that θ_{hkl} is the angle

between the diffracted beam and the planes. Further the incoming and diffracted beams must be in a plane normal to the set of diffracting planes. Once the diffraction angles 'θ' are measured, the corresponding d's and [hkl] values can be fixed. In the geometry of the practical diffractometers, only 2θ can be measured. So from the photographed X-ray pattern, the 2θ values and the intensity of the maxima can be found and a plot between 2θ and intensity made for studies. The modern X-ray diffractometers (XRD) make use of a built in computer, which is programmed to give directly the print out of a plot of 2θ versus intensity of the diffracted beam (Figure 1). The crystallite size was determined by means of the X-ray line broadening method using the Scherer equation.

$$D=\frac{0.94\,\lambda}{\beta\,\mathrm{Cos}\theta} \qquad (1)$$

Where, D, the crystallite size, λ, the wavelength of the radiation (1.5406Å for Cu-Kα radiation), β, the corrected peak width at half-maximum intensity, and θ, the peak position.

The calculated average crystallite size and its lattice parameters were tabulated in Tables 1 and 2 for the as-prepared sample and Tables 3 and 4 for 200°, for Li_2ZnCl_4 NPS which reveals the nanocrystalline size of the prepared powder. From this value, the specific surface area was calculated assuming the presence of spherical particles, by means of the equation.

$$S=\frac{6}{\rho\,D} \qquad (2)$$

Where, ρ, the calculated density of the material was nearly 2.536 g/cm^3 and D, the crystallite size of the sample. It has orthorhombic primitive lattices. From the Tables 1-4 the surface area of the particle 420 diffraction planes are different [10].

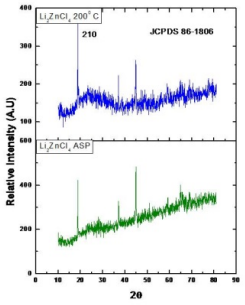

Figure 1: XRD analysis of Li_2ZnCl_4 for the asprepared and 200°C samples.

2Θ (obs)	2Θ(JCPDS) 86-1806	FWHM	dobs	Dexp (JCPDS) 86-1806	hkl	S=6/ρD
18.7955	18.314	0.1476	4.8404	4.7257	210	26
37.0806	37.118	0.1968	2.4202	2.4275	420	38
44.8714	44.873	0.1968	2.0182	2.0222	331	31

Table 1: Structural properties or the sample 5% concentration of Zn with Lithiumchloride aspreapred powdered particles.

hkl	Crystal Size (nm) $D=\frac{0.94\,\lambda}{\beta\,\mathrm{Cos}\theta}$	Lattice parameter (A°)			
210	54.8	A	b	c	
420	42.6	12.77	7.417	6.111	JCPDS
331	43.8	12.009	7.125	6.023	Calculated

Table 2: Crystal size and its lattice parameters for the sample 5% concentration of Zn with Lithium chloride for the as-prepared sample.

2Θ (obs)	2Θ(JCPDS) 86-1806	FWHM	dobs	dexp (JCPDS) 86-1806	$S=\frac{6}{\rho\,D}$
18.778	18.314	0.0984	4.7257	4.8404	63
37.0334	37.118	0.1476	2.4275	2.4202	56
44.8192	44.873	0.2460	2.0222	2.0182	58

Table 3: Structural properties for the sample 5% concentration of Zn with lithium chloride at 200°C.

hkl	Crystal Size	Lattice parameter (A°)			
210	81.21	A	b	c	
420	56.78	12.77	7.417	6.111	JCPDS
331	34.95	12.059	7.258	6.009	Calculated

Table 4: Crystal size and lattice parameters values for the sample 5% concentration of Zn with Lithiumchloride at 200°C.

SEM Analysis of Li_2ZnCl_4

Figure 2a and 2b shows the surface morphology of Li_2ZnCl_4 powdered particles prepared at proportions of (9:1) at room temperature for 1.0 Molar solution concentrations were observed. From these images it can be seen that the grain sizes of the powdered particles are not uniform. Therefore average grain sizes were estimated from different grains within the powder and to be about 0.8 μm to 1.0 μm. It is also seen that the edge texture of the particles become sharper and the grain boundaries become clearer by increasing the Zn content. It exhibits spherically shaped secondary particles consisting of primary nanospheres of approximately 0.8 μm to 1.0 μm [11].

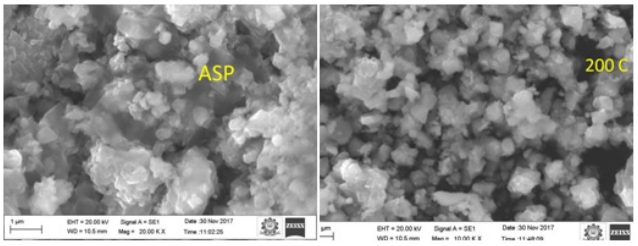

Figure 2a and 2b: Scanning Electron Microscopy and its analysis for ASP and 200°C.

Photoluminescence studies

The room temperature photo luminescent spectra of as prepared sample Li_2ZnCl_4 nano particles were studied using UV-excitation (λ=370 nm).The data were recorded in the region of 350 nm - 550 nm and spectra were shown in Figure 3. Li_2ZnCl_4 nano particles in the percentage of 0.05 equally were doped with Zn of 99% were dissolved in ethanol containing a weak UV emission at 493 nm (2.6 eV) and relatively intense emission at 532 nm (2.33 eV). The weak ultra violet emission at 494 nm is attributed to band edge emission which is associated with in the vacancy related to defects emission for 200°C sample. The medium intensity of other two peaks was due to the enhancement of non radioactive recombination process which occurred for the annealing samples [12].

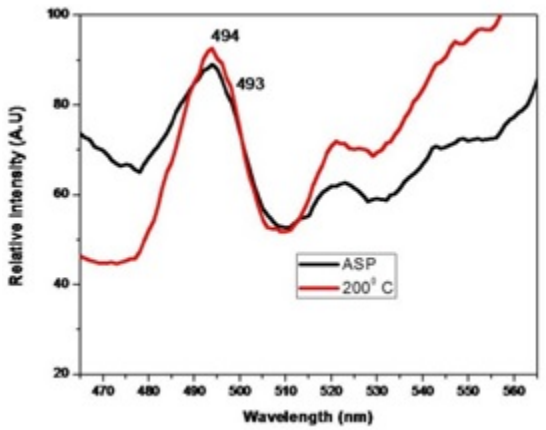

Figure 3: Photoluminescence analysis of Li_2ZnCl_4 NPs at ASP and at 200°C.

Conclusion

First time by simple co-precipitaton method Li_2ZnCl_4 NPs were prepared. The crystallite sizes for ASP and 200°C particles were calculated nearly equal to 47.06 nm and 57.64 nm the lattice parameter and dislocation densities were under the very small regimes. This is due to the small crystal size of the prepared particles. Due to its agglomeration the particle size becomes larger in μm shown in its morphological studies of Scanning Electron Microscopy. The PL analysis emission wavelength in nm well matched with the calculated prepared molar ratio of the source materials.

References

1. Nagatomo T, Maruta Y, Omoto O (1990) Electrical and optical properties of vacuum-evaporated indium-tin oxide films with high electron mobility. Thin Solid Films 192: 17-25.
2. Fallah HR, Ghasemi M, Hassanzadeh A, Steki H (2007) The effect of annealing on structural, electrical and optical properties of nanostructured ITO films prepared by e-beam evaporation. Mater Res Bull 42: 487-496.
3. Younggun H, Donghwan K, Jun-Sik C, Seok-Keun K (2005) Ultraflat indium tin oxide films prepared by ion beam sputtering. Thin Solid Films 473: 218-223.
4. Benamar E, Rami M, Messaudi C, Sayah D, Ennaoui A (1999) Structural, optical and electrical properties of indium tin oxide thin films prepared by spray pyrolysis. Solar Energy Materials and Solar Cells 56: 125-139.
5. Ellmer K (2000) Magnetron sputtering of transparent conductive zinc oxide: relation between the sputtering parameters and the electronic properties. J Phys D Appl Phys 33:R17-R32.
6. Kiyotaka W, Makoto K, Adachi (2004) Thin Film Materials Technology Sputtering of Compound Materials. (1stedn), William Andrew, USA.
7. Ellerby LM, Nishida CR, Nishida F, Yamanaka SA, Dunn B, et al. (1992) Encapsulation of proteins in transparent porous silicate glasses prepared by the sol-gel method. Science 255: 1113-1115.
8. Jianbo L, Yong F, Hua P, Meiqiang F, Liangliang W, et al. (2012) Controllable hydrogen generation performance from Al/NaBH4 composite activated by La metal and CoCl2 salt in pure water. Journal of Rare Earths 30: 548-551.
9. Bardeen J (1947) Surface states and rectification at a metal semiconductor contact. Phys Rev 71: 717.
10. Liu S, Bao HB, Fan M, Chen D, Shu KY (2001) Study on hydrogen generation from AlLi/NaBH4 mixture in pure water for portable fuel cell. Adv Mater Res 239: 1058-1061.
11. Xing RU, Whitman WB (1994) Purification and characterization of the oxygen-sensitive acetohydroxy acid synthase from the archaebacterium Methanococcus aeolicus, J bacteriol 176: 1207-1213.
12. Paro L, Guglielmin M (2011) FINAL REPORT Handbook to establish alpine permafrost monitoring network. Italy.